Sakarya Üniversitesi Fen Bilimleri Dergisi
Sakarya University Journal of Science

e-ISSN : 2147-835X
Publisher : Sakarya University

Vol. x, No. x, xx-xx, 202x
DOI: https://doi.org/10.16984/saufenbilder.xxxxxx

Research Article

Performance Evaluation of Polypropylene Recycled Fibers in Concrete

Abdul Samed Demirhan[1], Aylin Özodabaş[2]

[1] Bilecik Şeyh Edebali University, Faculty of Engineering, Department of Civil Engineering, Bilecik, Türkiye, E-mail: sameddemirhan@gmail.com, ORCID: 0009-0000-2472-5194
[2] Bilecik Şeyh Edebali University, Faculty of Engineering, Department of Civil Engineering, Bilecik, Türkiye, E-mail: aylin.ozodabas@bilecik.edu.tr, ORCID: 0000-0002-6011-980X
[2] Corresponding Author: aylin.ozodabas@bilecik.edu.tr

ARTICLE INFO

Keywords:
Recycled fibers
Polypropylene fibers
Fiber-reinforced concrete
Mechanical properties
Sustainability

Article History:
Received: xx.xx.202x
Revised: xx.xx.202x
Accepted: xx.xx.202x
Online Available: xx.xx.202x

ABSTRACT

Recycled granules are obtained from the waste materials generated during the production of polypropylene macro synthetic fibers (PF) used in concrete. In this study, PF were obtained again from these granules, and their reuse as fiber reinforcement in concrete is proposed. The main objective of this approach is to evaluate the mechanical and structural performance of concrete containing recycled polypropylene fibers (RPF) and to provide a cost-effective and environmentally sustainable solution.The experimental program includes the evaluation of fundamental mechanical properties such as tensile strength and elastic modulus. Furthermore, the structural performance of PF and RPF reinforced concrete will be evaluated according to the EN 14651 standard, focusing particularly on load-CMOD (Crack Opening Displacement) behavior, fracture energy (Fr), and bending moment capacity. Additionally, SEM analyses were conducted to provide insight into the fiber distribution and fiber-matrix interactions within the concrete matrix.

1. Introduction

In recent decades, concrete has remained the predominant material in construction due to its high compressive strength, availability, and versatility. However, its inherent weaknesses, notably low tensile strength and brittle post-cracking behavior, have necessitated enhancements via fiber reinforcement. Among fiber-reinforced concretes (FRCs), macro-synthetic fibers (e.g., polypropylene, polyethylene terephthalate) have been adopted widely for improving crack control, toughness, and ductility [1]. Synthetic fiber reinforcement provides a three-dimensional distribution within the concrete, increasing tensile strength and improving crack resistance. Thanks to their homogeneous distribution in the concrete matrix, they bridge micro cracks that may occur and prevent their widening. By being resistant to corrosion, they enhance the durability performance of concrete and contribute to the production of long-lasting concrete structures [2]. Simultaneously, environmental concerns—such as resource depletion, energy consumption, and greenhouse gas emissions—plus waste management challenges have driven the construction materials community toward more sustainable solutions. The reuse of industrial by-products and waste materials in concrete is emerging as a promising route to reduce environmental impact while maintaining or improving mechanical performance.

Cite as: N. Surname, N. Surname, "Manuscript title, write in times new roman 12 point size, only the first letter of the first word should be capitalised," Sakarya University Journal of Science, vol. xx, no. xx, pp. xx-xx, 202x. https://doi.org/10.16984/saufenbilder.xxxxxx

Recycled synthetic fibers, particularly, offer potential not only in reducing waste but also in substituting virgin fibers in concrete applications [3, 4]. Therefore, as shown by recent reviews, there is increasing interest in using recycled fibers (mainly steel and polymeric fibers) in FRC [5-7].

Recent literatures demonstrate that incorporating recycled synthetic fibers into concrete can enhance flexural, tensile, and sometimes compressive properties, under certain fiber dosages. For example, a critical review noted that up to ~2% fiber volume (by concrete volume) yields improvements in strength and toughness, while higher dosages often lead to adverse effects on workability and sometimes on mechanical behavior [8-11]. Moreover, fully-recycled plastic macro-fibers have been shown to significantly improve energy dissipation (post-cracking behavior) and peak strength under flexural, provided that fiber–matrix bonding and fiber geometry are optimized [12, 13]. Another study determined the optimum fiber content by adding 0.5% Polyethylene Terephthalate fiber to cement by weight, significantly improving crack control and ductility [14]. These studies show that it is possible to reprocess waste fibers and make them usable, and that this provides environmental benefits [15].

In response to the growing demand for both structural performance and sustainability in construction materials, this study explores the potential of utilizing recycled fibers derived from macro-synthetic fiber waste as reinforcement in concrete [16]. Recycled macro- polypropylene fibers increased the tensile strength performance in concrete by 41.9% [17]. Not only polypropylene but also synthetic polymers such as polyethylene have shown that adding recycled polyethylene fibers to concrete improves the tensile strength and crack resistance of concrete, increasing environmental sustainability [18]. These wastes, originally left over from the production or processing of macro-synthetic fibers [19] used in concrete, are first granulated and then reprocessed into fiber form with consistent geometry. This engineered two-step recycling approach aims to enhance the compatibility of the recycled fibers with the cementitious matrix, while also promoting uniform dispersion within the concrete mix.

The overarching goal of the research is to evaluate whether these recycled fibers can serve as a viable alternative to virgin synthetic fibers, which are traditionally used in their pure, unprocessed form. A comprehensive comparison is conducted between concretes reinforced with virgin fibers and those incorporating recycled fibers, focusing on key mechanical properties such as tensile strength and modulus of elasticity. Structural performance is assessed through residual flexural strength and moment capacity testing, in accordance with the EN 14651 standard [20]. Furthermore, microstructural analyses are carried out to investigate fiber–matrix interactions, fiber morphology, and the presence of micro-defects potentially introduced during the recycling process.

By eliminating the risk of corrosion inherent in traditional steel reinforcements, these PF especially in their recycled form are expected to contribute to improved durability and facilitate the production of longer-lasting, more sustainable concrete structures. Ultimately, this study seeks to demonstrate that the controlled reintegration of PF waste into concrete offers not only offers environmental and economic benefits while maintaining structural integrity and long-term performance.

2. Materials and Methods

2.1. Materials

Aggregate

Aggregates used in the experiments were obtained from the aggregate facilities of Bilecik Oz Dag Is Concrete. Three different aggregate types were used: 0-0.5 mm (crushed stone dust), 4-16 mm No. 1 (natural gravel), and 16-32 mm No. 2 (crushed stone). Aggregate granulometry curve standards were determined according to TS 706.

Cement

CEM II 42.5 R Portland cement from Çimsa company was used.

Fiber

PF obtained from Company A was used. The properties of the fibers used are given in Table 1 (The data were obtained from the Polyfibers). The recycling of PF waste into reusable granules is primarily based on mechanical recycling processes. Initially, RPF is collected and carefully sorted to ensure polymer homogeneity, as the presence of mixed polymers negatively affects the quality of recycled products. The sorted material is then washed to remove surface contaminants such as dirt and oils, followed by shredding into flakes to facilitate uniform melting. These flakes are subsequently melted and extruded under controlled conditions, and the resulting polymer strands are cooled and pelletized into RPF granules. The obtained granules can be used directly or blended with PF, with quality verified through standard tests such as melt flow index and mechanical performance evaluation. This process contributes to sustainable material management by promoting circular use of PF and reducing environmental burdens associated with plastic waste [21].

Table 1. Physical and mechanical properties of PF fibers

		PF	
Medicine	Macro fiber twist form	**Fiber Count**	100,000+/kg
Available Lengths	Standard 54 mm	**Corrosion**	None
Length/Width ratio	112	**Absorption**	Non-absorptive
Colour	White or gray	**Chemical Resistance**	Alkali resistance
Specific gravity	0.91gr / cm³	**Magnetism**	Antimagnetic
Elasticity Module	5.0-5.5 GPa	**Melting Point**	165° C
Pull Strength	600-650 MPa	**Combustion Point**	>360° C

Concrete Additive

Floor Grade® S 37 brand was used as an additive in concrete production. It is a high-performance concrete additive that gives concrete high fluidity and increases strength by providing this fluidity with less water. The admixture complies with the TS EN 934-2 standard [22] and is free from calcium chloride. It was used at a dosage of 1% by weight of cement, and its characteristics are presented in Table 2 (The data were obtained from the Polyfibers Company). The codes, PF amounts and mixing ratios of the samples used in concrete are presented in Table 3. The contents in Table 3 are given in kg (weight).

Table 2. Chemical and physical properties of the additive material used

Form	Homogeneous, Liquid
Colour	Brown
Density (20°C)	1.050 ± 0.020 g/cm3 (TS 781 ISO 758)
pH (20°C)	5.0 ± 1.5 (TS 6365 EN 1262)
Total Chlorine Amount:	<0.10 M.-% (TS 1116 EN ISO 1158)
Amount of Chlorine Dissolved in Water	<0.10 M.-% (TS EN 480-10)
Alkali amount:	<7.0 M.-% (TS EN 480-12)
Recommended dosage	0.5-2.0% of the total binder amount

Table 3. Mixing ratios of materials used in concrete

Specimens code	Cement	Fine aggregate (0-4 mm)	Aggregate (4-11 mm)	Aggregate (11-22 mm)	Superplasticizer	PF	RFP
R*	320	916.2	374.8	564.3	3.2		
F0-2	320	916.2	374.8	564.3	3.2	2	0
F0-3	320	916.2	374.8	564.3	3.2	3	0
F5-2	320	916.2	374.8	564.3	3.2	1.90	0.10
F5-3	320	916.2	374.8	564.3	3.2	2.85	0.15
F10-2	320	916.2	374.8	564.3	3.2	1.80	0.20
F10-3	320	916.2	374.8	564.3	3.2	2.70	0.30
F15-2	320	916.2	374.8	564.3	3.2	1.70	0.30
F15-3	320	916.2	374.8	564.3	3.2	2.55	0.45

*R: Fiber-free reference sample

2.2. Methods

The concrete used in the study is class C30/37. The slump value used in the calculation was kept high because the mixture contained fibers, and was taken as 20 cm for reference concrete.

In the produced concrete specimens, fresh concrete tests such as fresh unit weight, air content determination, and slump flow were conducted, while hardened concrete was

subjected to flexural strength, compressive strength, and microstructural analysis tests. The tests were conducted using the concrete laboratory at the Polipropilen Elyaf ve Dış Tic. A.Ş. plant.

Fresh concrete tests

The slump test was performed on the prepared concrete in accordance with the TS EN 12350-2 [23] standard.

To determine the fresh concrete unit weight, the prepared concrete specimens were measured using an 8 dm^3 unit volume container and a laboratory balance with a precision of 5 g to determine the air content, the concrete was placed in an air meter container in three stages. At each stage, it was rammed 25 times by its own weight and compacted with a tamper. After the final layer was applied, the surface was smoothed with a trowel. The concrete placed in the air meter container was filled with water by opening two opposite valves. When water was observed escaping from the opposite valve, the valves were closed, releasing the pressure. The air content was determined in this manner (Figure 1).

Figure 1. Concretes prepared for determination of fresh concrete unit volume weight

2.2.1. Hardened concrete tests

Concrete specimens were prepared using a metal mixer and poured into molds (60*15*15 cm) in three layers, with each layer compacted by rodding 25 times. Once the molds were completely filled, they were placed on a vibrating table to eliminate any entrapped air. After vibration, the surface was topped off with concrete and finished using a steel trowel. The specimens were demolded after 24 hours and then placed in a curing tank. Following a 28-day curing period, the specimens were tested for compressive strength using a concrete compression testing machine, as illustrated in Figure 2. For each concrete series, four cube specimens measuring 150 × 150 × 150 mm were produced to ensure compliance with the TS 3114 [24] standard for compressive strength evaluation.

Figure 2. Compressive strength test

According to the EN-14651 standard specimens shall be rotated over 90° around their longitudinal axis and then sawn through the width of specimen at mid-span. As illustrated in Figure 3, the area marked as (1) represents the top surface during casting, (2) indicates the notch location, and (3) shows the cross-section of the test specimen. As in Figure 3, the notch width should be 5 mm or less, and the distance between the tip of the notch and the top of the test specimen in the mid-span section (hsp) distance should be 125 mm ± 1 mm.

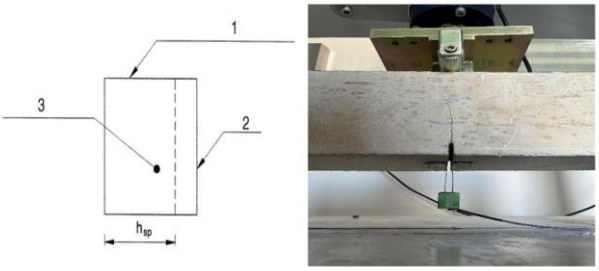

Figure 3. Flexural test setup, notch location, and crack mouth opening displacement (CMOD) gauge

2.2.2. Proportionality limit

The limit of proportionality (LOP) is an important parameter in determining the mechanical performance of fiber-reinforced concrete and is determined by three-point flexural tests performed on notched prismatic

specimens. LOP is defined as the stress at the notch tip, and this stress is assumed to act in the cross-section at the midpoint where cracking does not occur. The key variables in the formula used for this calculation are fct, L (limit of proportionality stress), F_L (load at limit of proportionality), l (support span), b (specimen width), and hsp (distance between the notch tip and the top elevation of the flexural specimen). According to the EN-14651 standard, the calculation of fct, LOP is as follows.

$$f\mathrm{ct,L} = (3.\mathrm{FL}.\mathrm{l}) \div (2.\mathrm{b}.\mathrm{hsp}^2) \qquad (2.1)$$

The F_L load value at the proportionality limit is measured using the crack opening displacement (CMOD) graph. During this process, a line parallel to the load axis is drawn on the CMOD graph at a distance of 0.05 mm. The maximum load value between this line and the load CMOD curve on the graph is accepted as the F_L for the proportionality limit. This method allows for precise determination of the LOP.

Residual Flexural Tensile Strength

The residual flexural tensile strength is calculated using the formula:

$$f_{R,j}=(3.Fj.l) / (2.b.\ hsp^2) \qquad (2.2)$$

Here, $f_{R,j}$ is the residual flexural tensile strength, Fj is the residual flexural tensile strength at crack opening values, l is the support span, b is the specimen width, and hsp is the distance between the notch tip and the top of the specimen. The recorded load value at the crack opening values ($CMOD_j$) is shown schematically in Figure 4. F_J values are shown from a typical fiber-reinforced concrete load-CMOD graph with a specific fiber dosage. In the Figure 4 graph, F1 shown on the Y-axis represents the load value at a crack opening of CMOD1 = 0.5 mm, F2 represents the load value at a crack opening of CMOD2 = 1.5 mm, F3 represents the load value at a crack opening of CMOD3 = 2.5 mm, and F4 represents the load value at a crack opening of CMOD4 = 3.5 mm.

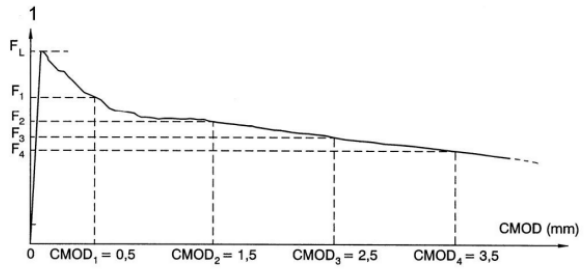

Figure 4. Load-CMOD diagram and $F_{J\ (j = 1, 2, 3, 4)}$ (EN 14651)

2.2.3. Test procedure

In the central cross-section of the specimen, the distance between the notch tip and the top surface, as well as the average width of the specimen, are determined using a caliper. These measurements are taken at the notched section with a maximum precision of 0.1 mm from two different points.

If the crack (or notch) mouth opening displacement is to be measured, a displacement transducer should be mounted at the mid-width of the specimen along the longitudinal axis. The vertical distance (y) between the measurement line and the bottom of the specimen must be 5 mm or less.

Loading must begin only after all rollers uniformly contact the specimen. If a CMOD-controlled device is used, CMOD should increase at 0.05 mm/min, then 0.2 mm/min after reaching 0.1 mm. Load and CMOD should be recorded at ≥5 Hz for the first 2 minutes, and ≥1 Hz thereafter, continuing until CMOD ≥ 4 mm. If the minimum load between $CMOD_{FL}$ and 0.5 mm is <30% of the load at 0.5 mm, the procedure should be checked for instability. Deflection-controlled tests may be used if CMOD parameters are appropriately converted. Tests with cracks initiating outside the notch are invalid

3. Results and Discussion

3.1. Slump test

In the slump test, the measured slump value for the reference concrete (R) was 20 cm, while it decreased to 17 cm for the mix containing 2 kg/m³ of fiber (A), and to 15 cm for the mix with

3 kg/m³ of fiber (B). This reduction in slump is attributed to the presence of fibers, which help hold the concrete matrix together, resulting in lower flowability compared to the reference mix (Figure 5) [25].

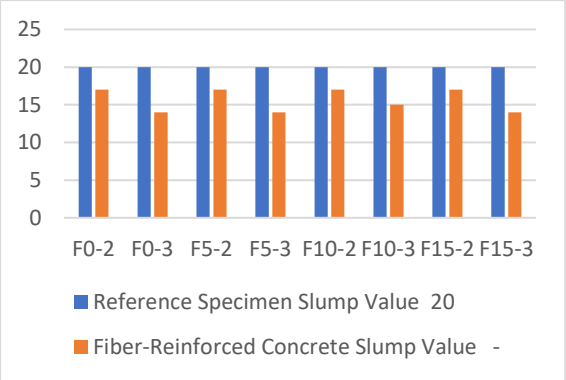

Figure 5. Slump Values

3.2. Compressive test

The fibers we used contain more than 100,000 filaments per kilogram. Although the highest strength value was observed in the F15-2 specimen, the reference specimen generally exhibits higher compressive strength compared to the other specimens. This can be attributed to the absence of fibers—and therefore filaments—in the concrete, which prevents the formation of voids within the matrix. As shown in Figure 6, the reference specimen demonstrates the highest compressive strength. In general, as the fiber dosage increases, the compressive strength tends to decrease; however, this reduction is negligible at low dosage levels.

In the other study conducted, mixtures containing a fiber dosage of 4 kg/m³ were compared with plain concrete; the highest compressive strength, 55.8 MPa, was obtained for the plain concrete, followed by 52.5 MPa for the mixture reinforced with virgin PP fibers. These results indicate that fiber addition may have a limited and generally adverse effect on the compressive strength of concrete.

The compressive strength results obtained in the present study exhibit a similar trend. Compared to plain concrete, PP fiber-reinforced concretes showed a reduction in compressive strength, which can be attributed to the high filament count of the fibers, leading to the formation of local voids within the concrete matrix and discontinuities at the fiber–matrix interface [26].

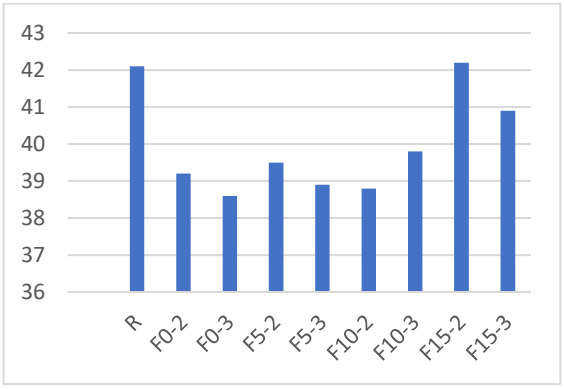

Figure 6. Cube Compressive Strength

3.3. Calculation of moment capacity from notched beam and tests flexural test

Based on notched beam tests performed according to the EN 14651 standard, the values of fR1 (stress at 0.5 mm crack opening) and fR4 (stress at 3.5 mm crack opening) were obtained. Using these values, the average axial tensile strengths were calculated as;

$$\sigma r1 = 0.45 \times fR1 \quad (3.1)$$
$$\sigma r4 = 0.37 \times fR4 \quad (3.2)$$

At the ultimate limit state, it is assumed that the axial tensile strength at the crack tip is σr1, and that the tensile stress distribution at the crack surface follows a triangular shape with a maximum of σr4. The stress block in fiber-reinforced concrete is illustrated in Figure 7.

The ultimate moment capacity of an in-situ concrete slab, with thickness h and material safety factor γm, is calculated using the formula:

$$Mu = h^2 \times (0.29\sigma r4 + 0.16\sigma r1) / \gamma m. \quad (3.3)$$

Since the slab thickness and safety factor remain constant for the same concrete slab, the moment coefficient (MCC) can be simplified as:

$$MCC = 0.29\sigma r4 + 0.16\sigma r1. \quad (3.4)$$

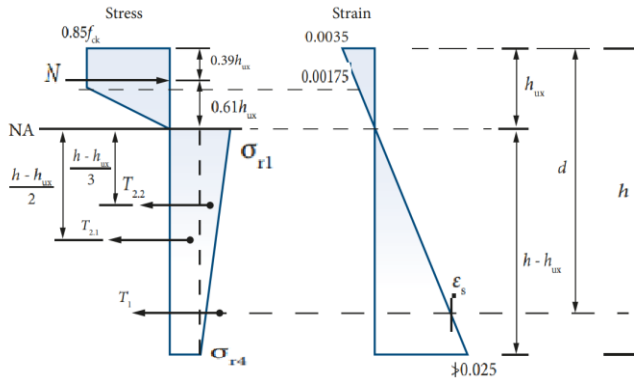

Figure 7. Tension block in fiber reinforced concrete (Technical Report 34

According to the EN 14651 test standard, six beam specimens were prepared for each series (R, F0-2, F0-3, F5-2, F5-3, F10-2, F10-3, F15-2 and F15-3), and tested for flexural performance after 28 days.

The Moment Calculation Coefficient (MCC) was calculated using the fr1 and fr4 values of the fractured specimens, due to the same specimen (h and γ_m are constant), and the load CMOD graphs are shown.

The CMOD and MCC values reference (R) obtained from the fractured specimens and the change in load CMOD are shown in Figure 8. After R fractures, the graph suddenly drops to zero because there is no reinforcement to bridge the crack. R concrete has no crack-bridging or crack-limiting properties.

In Figure 8, Flexural tests performed in accordance with EN 14651 demonstrated that both fiber dosage and RPF granule content significantly influence the post-cracking behavior of concrete. As illustrated in Figure 8, increasing fiber dosage improves mechanical performance, whereas increasing granule content generally leads to a reduction in post-cracking strength.

The reference concrete without fibers (Figure 8a, R) exhibited very low post-cracking strength (fR1 ≈ 0.5 MPa). All fiber-reinforced mixtures (Figures 8b–8i) showed substantial improvements. Compared to the reference mix, fR1 increased by approximately 180% for F0-2 (Figure 8b), 200% for F0-3 (Figure 8c), and between 140% and 200% for the mixtures containing 5% granules (Figures 8d and 8e). These results confirm that even low fiber dosages increase post-cracking strength by approximately 2–3 times.

Effect of fiber dosage; In granule-free mixtures (Figures 8b and 8c: F0-2 and F0-3), increasing the fiber dosage from 2 to 3 kg/m³ resulted in increases of 7% in fR1, 36% in fR3, and 28% in moment capacity. The pronounced improvement in fR3 at CMOD = 2.5 mm (Figure 8c) highlights the positive effect of higher fiber content on energy absorption capacity at advanced crack openings.

A similar trend was observed in granule-containing mixtures. For mixtures with 5% granule content (Figures 8d and 8e), increasing the fiber dosage improved fR1 and fR3 by approximately 25% and 33%, respectively. For higher granule contents (Figures 8f–8i), increasing fiber dosage partially compensated for performance losses; however, overall strength remained lower than that of mixtures with lower granule contents.

Effect of granule content; at a constant fiber dosage, increasing the recycled granule content led to a gradual decrease in post-cracking performance. For mixtures with 2 kg/m³ fiber (Figures 8b, 8d, 8f, and 8h), reductions of 14–21% in fR1 and 14–29% in fR3 were observed as granule content increased from 0% to 15%. For mixtures with 3kg/m³ fiber (Figures 8c, 8e, 8g, and 8i), the reductions were less pronounced, with maximum decreases of 13% in fR1 and 26% in fR3. This indicates that higher fiber dosages effectively mitigate granule-induced bond degradation, although performance losses become unavoidable at granule contents of 10% and above. Increasing the fiber dosage from 2 to 3 kg/m³ enhances post-cracking strength by approximately 20–50%, while increasing recycled granule content from 0% to 15% reduces performance by about 15–30% (Figure 8). Considering both mechanical performance and sustainability, the mixture containing 5% RPF granules and 3 kg/m³ fiber (Figure 8e, F05-3) provides the most balanced solution. The highest mechanical performance was achieved by the granule-free mixture with 3 kg/m³ fiber (Figure 8c, F0-3) [27].

R	Proportional Limit	CMOD= 0,5 mm	CMOD = 1,5mm	CMOD = 2,5mm	CMOD = 3,5mm	Moment calculation coefficient
	fcti, Mpa	f_{r1}, Mpa	F_{r2}, Mpa	F_{r3}, Mpa	F_{r4}, Mpa	
Average	4,7	0,5	0,0	0,0	0,0	0,03

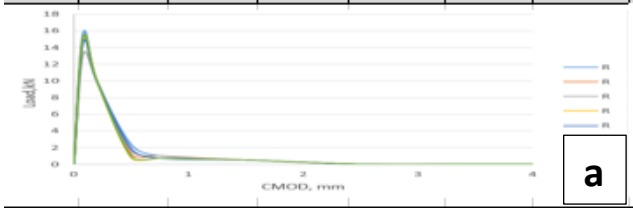

a

F05-2	Proportional Limit	CMOD= 0,5 mm	CMOD = 1,5mm	CMOD = 2,5mm	CMOD = 3,5mm	Moment calculation coefficient
	fcti, Mpa	f_{r1}, Mpa	F_{r2}, Mpa	F_{r3}, Mpa	F_{r4}, Mpa	
Average	5,1	1,2	1,1	1,2	1,2	0,22

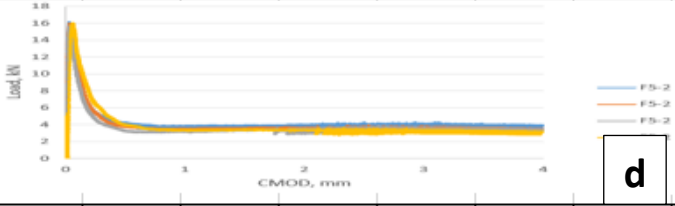

d

F10-3	Proportional Limit	CMOD= 0,5 mm	CMOD = 1,5mm	CMOD = 2,5mm	CMOD = 3,5mm	Moment calculation coefficient
	fcti, Mpa	f_{r1}, Mpa	F_{r2}, Mpa	F_{r3}, Mpa	F_{r4}, Mpa	
Average	4,8	1,3	1,4	1,5	1,6	0,26

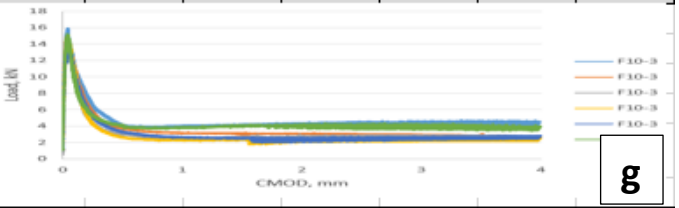

g

F0-2	Proportional Limit	CMOD= 0,5 mm	CMOD = 1,5mm	CMOD = 1,5mm	CMOD = 3,5mm	Moment calculation coefficient
	fcti, Mpa	f_{r1}, Mpa	F_{r2}, Mpa	F_{r3}, Mpa	F_{r4}, Mpa	
Average	4,7	1,4	1,3	1,4	1,4	0,25

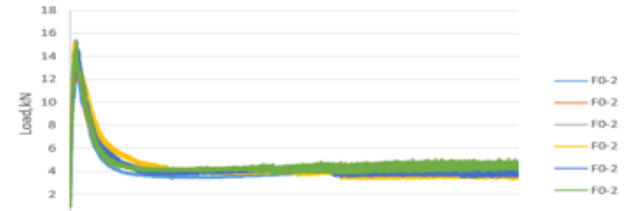

b

F05-3	Proportional Limit	CMOD= 0,5 mm	CMOD = 1,5mm	CMOD = 1,5mm	CMOD = 3,5mm	Moment calculation coefficient
	fcti, Mpa	f_{r1}, Mpa	F_{r2}, Mpa	F_{r3}, Mpa	F_{r4}, Mpa	
Average	5,0	1,5	1,7	1,8	1,8	0,30

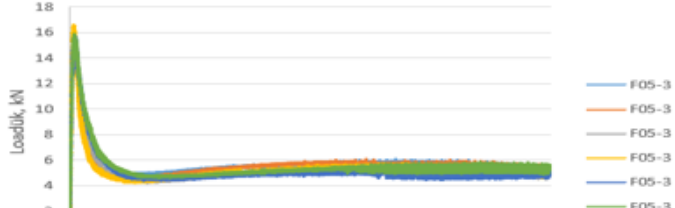

e

F15-2	Proportional Limit	CMOD= 0,5 mm	CMOD = 1,5mm	CMOD = 2,5mm	CMOD = 3,5mm	Moment calculation coefficient
	fcti, Mpa	f_{r1}, Mpa	F_{r2}, Mpa	F_{r3}, Mpa	F_{r4}, Mpa	
Average	4,9	1,1	0,9	1,0	1,0	0,18

h

F0-3	Proportional Limit	CMOD= 0,5 mm	CMOD = 1,5mm	CMOD = 1,5mm	CMOD = 3,5mm	Moment calculation coefficient
	fcti, Mpa	f_{r1}, Mpa	F_{r2}, Mpa	F_{r3}, Mpa	F_{r4}, Mpa	
Average	4,4	1,5	1,7	1,9	1,9	0,32

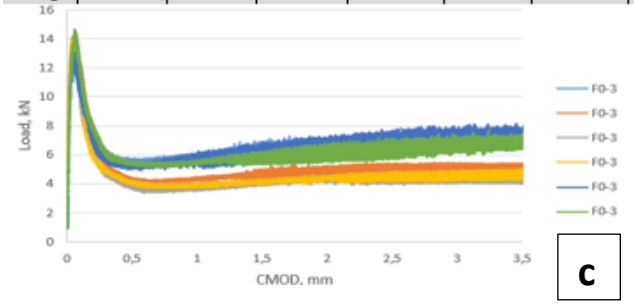

c

F10-2	Proportional Limit	CMOD= 0,5 mm	CMOD = 1,5mm	CMOD = 2,5mm	CMOD = 3,5mm	Moment calculation coefficient
	fcti, Mpa	f_{r1}, Mpa	F_{r2}, Mpa	F_{r3}, Mpa	F_{r4}, Mpa	
Average	4,7	1,1	0,9	1,0	1,0	0,18

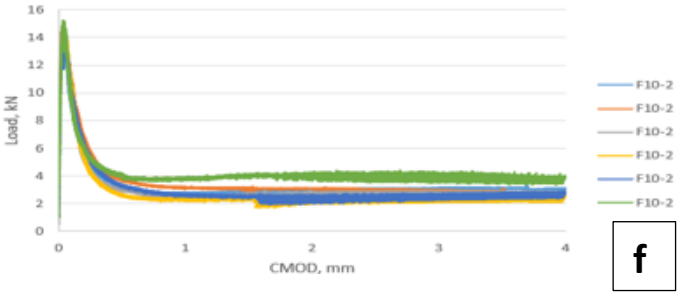

f

F15-3	Proportional Limit	CMOD= 0,5 mm	CMOD = 1,5mm	CMOD = 2,5mm	CMOD = 3,5mm	Moment calculation coefficient
	fcti, Mpa	f_{r1}, Mpa	F_{r2}, Mpa	F_{r3}, Mpa	F_{r4}, Mpa	
Average	4,6	1,3	1,3	1,3	1,4	0,24

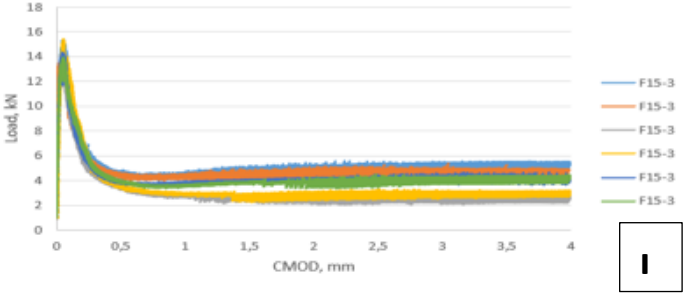

ı

Figure 8.a) Reference(without fibers) MCC values and CMOD- load chart, b) F0-2 MCC values and CMOD- load chart, c) F0-3 MCC values and CMOD- load chart, d) F05-2 MCC values and CMOD- load chart, e) F05-3 MCC values and CMOD- load chart, f) F10-2 MCC values and CMOD- load chart, g)F10-3 MCC values and CMOD- load chart, h) F15-2 MCC values and CMOD- load chart, ı) F15-3 MCC values and CMOD- load chart

The graphs corresponding to the fR1, fR4, and MCC parameters presented in Figure 8 are illustrated in detail in Figure 9, where a pronounced decreasing trend is observed in all parameters with increasing RPF content.

A comparison of the flexural performance of concrete reinforced with PF and RPF fibers indicates that mixtures incorporating recycled polymer granules exhibit lower residual flexural strength than those reinforced with virgin PP fibers. This reduction in residual strength can be attributed to the comparatively inferior mechanical properties and bonding characteristics of recycled polymer materials. Similar observations have been reported in EN 14651 flexural tests conducted on 40 MPa concrete, where mixtures containing 0.67% recycled PP fibers demonstrated noticeably lower residual strength values. This decrease in performance became more pronounced at higher CMOD levels, indicating a reduced ability of the fibers to effectively bridge cracks as crack openings increased. In addition to the loss in residual strength, a corresponding reduction in moment-carrying capacity was also observed, highlighting the influence of fiber quality on structural performance.

The results of the present study are consistent with these previously reported findings, confirming the trends observed in the literature. Although all fiber-reinforced mixtures exhibited significant improvements in post-cracking behavior when compared to the reference concrete, variations in fiber type and composition led to notable differences in performance. The highest fR1 and fR3 values were obtained from the granule-free mixture with a fiber dosage of 3 kg/m³, indicating the superior efficiency of virgin fibers in enhancing flexural response. Increasing the fiber dosage generally resulted in improved post-cracking performance due to enhanced crack-bridging capacity and energy absorption.

Conversely, increasing the recycled granule content caused a gradual reduction in residual strength, reflecting the trade-off between sustainability and mechanical efficiency. Overall, limiting the recycled granule content to approximately 5% appears to offer a balanced compromise between maintaining adequate mechanical performance and achieving sustainability objectives [28].

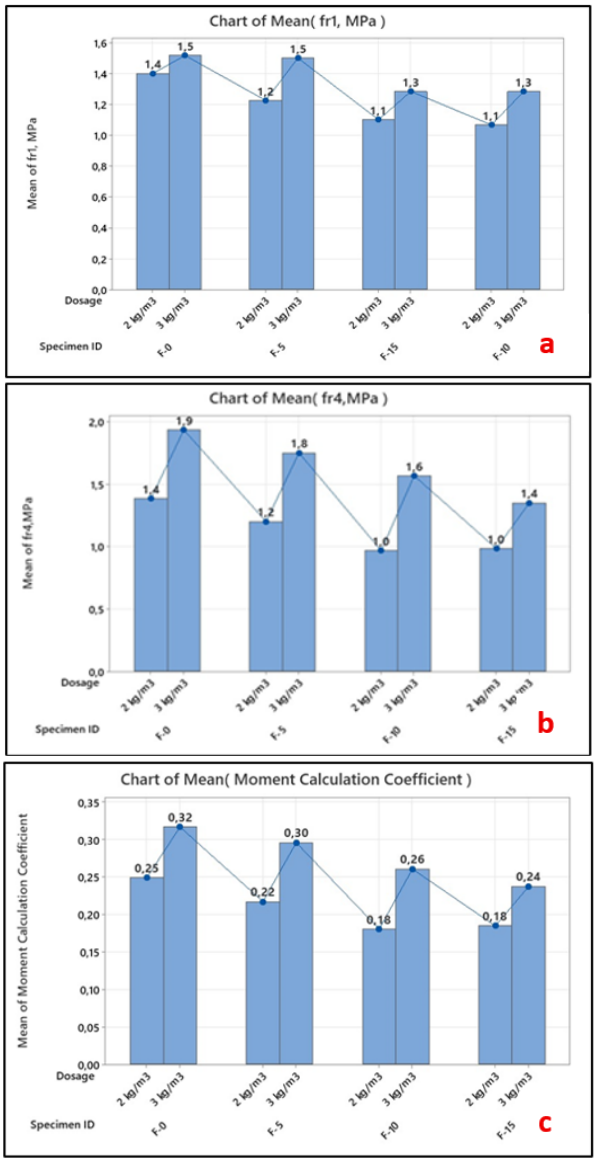

Figure 9. Average a) fR1, b) fR4 and c) Moment Calculation Coefficient, MPa values

3.4. Characterization of tensile and elongation performance of yarn

The ISO 2062 standard [34] defines the method for determining the tensile strength and elongation at break of yarns using a single-end tensile test with a constant rate of extension (CRE) testing machine. In this method, yarn specimens are conditioned under standard atmospheric conditions (20 ± 2 °C temperature and 65 ± 4% relative humidity), clamped at a specified gauge length, and stretched at a constant speed until breakage. The device automatically records the maximum breaking force, elongation, and stress-strain data. In this

study, tests were carried out using a Zwick Roell device in accordance with ISO 2062:2009 (CRE method, see Figure 10) to evaluate the mechanical performance of PF yarns containing various amounts of recycled content.

Yarn samples were prepared with 0% (F-0), 5% (F-5), 10% (F-10), and 15% (F-15) RPF granules. These tables present the results of yarn tensile strength tests performed in accordance with ISO 2062.

The purpose of the tests was to evaluate the effect of RPF granule content on the mechanical properties of the yarns.

The yarns were produced by incorporating 0%, 5%, 10%, and 5% recycled granules, respectively. Each table shows the average values of maximum tensile force (F_{max}), specific strength (σ/den), elongation at break (dL at F_{max}), titer, and elastic modulus ($E_{mo}d$) for the corresponding granule ratio.

Series "a" and "b" represent repeated measurements for the same yarn type, ensuring the repeatability and reliability of the results.

According to the data, as the granule content increases, a gradual decrease in tensile strength (F_{max}) and elastic modulus ($E_{mo}d$) is observed. This trend indicates that higher granule content slightly reduces the molecular alignment and inter-fiber bonding within the yarn structure. However, the elongation at break values remains relatively stable, suggesting that the ductility of the yarns is largely preserved.

Based on the results presented in Table 4 and Table 5 and Figure 20, the yarn test results conducted in accordance with the ISO 2062 standard indicate that the tensile strength and elastic modulus decreased with increasing recycled content. F-0 exhibited values of 650 MPa and 8.5 GPa, while F-5 showed 630 MPa and 8.2 GPa. For F-10, these values decreased to 600 MPa and 8.0 GPa, and F-15 recorded the lowest values of 590 MPa and 7.9 GPa. These trends are also illustrated in Figure 11. The reduction in mechanical properties is attributed to molecular degradation, shorter polymer chain lengths, and reduced crystallinity resulting from the incorporation of recycled material.

The tensile strength and elastic modulus decreased with increasing recycled content: F-0 exhibited 650 MPa and 8.5 GPa, F-5 had 630 MPa and 8.2 GPa, F-10 showed 600 MPa and 8.0 GPa, and F-15 recorded 590 MPa and 7.9 GPa. These trends are also illustrated in the reduction in mechanical properties is attributed to molecular degradation, shorter polymer chains, and lower crystallinity due to the addition of recycled material [29].

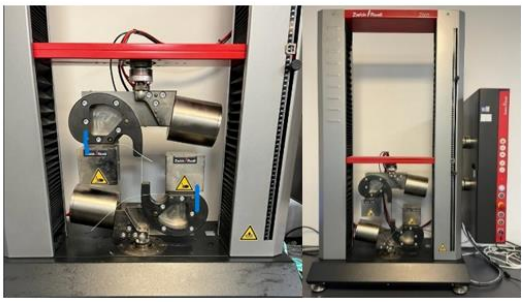

Figure 10. Yarn tensile test according to ISO 2062:2009 standard CRE m

Table 4. Results of a) F-0 and b) F-5 yarn samples according to ISO 2062 standard

Legend	No.	F_{max} N	F_{max} kg	σ g/den	σ MPa	dL at F_{max} %	Titer den	t_{test} s	E_{mod} GPa	E_{mod}(10-30F_{max}) GPa
	1	2560	260,79	8,69	643,37	10,6	30000	11,10	9,40	8,39
	2	2510	255,69	8,52	654,18	10,5	30000	10,99	9,34	8,44
	3	2510	256,43	8,55	635,19	10,3	30000	10,90	9,66	8,29
	4	2520	256,59	8,55	639,45	10,8	30000	11,25	9,13	8,35
	5	2530	257,64	8,59	664,33	10,8	30000	11,25	9,29	8,69
	6	2500	255,26	8,51	645,70	10,5	30000	10,99	9,45	8,44
	7	2480	252,69	8,42	65382	10,5	30000	10,97	9,03	8,57
	8	2500	255,14	8,50	665,24	10,4	30000	10,94	9,10	8,64
	9	2520	256,60	8,55	643,11	10,6	30000	11,09	9,26	8,43
	10	2550	259,80	8,66	655,40	10,7	30000	11,2 4	9,17	8,57

Statistics:

Series n = 10	F_{max} N	F_{max} kg	σ g/den	σ MPa	dL at F_{max} %	Titer den	t_{test} s	E_{mod} GPa	E_{mod}(10-30F_{max}) GPa
$\bar{x}$	2520	256,66	8,56	649,98	10,6	30000	11,07	9,28	8,48
s	22,8	2,33	0,08	6,24	0,2	0,000	0,13	0,189	0,17
V [%]	0,91	0,91	0,91	0,91	1,51	0,00	1,22	2,03	2,05

a

Legend	No.	F_{max} N	F_{max} kg	σ g/den	σ MPa	dL at F_{max} %	Titer den	t_{test} s	E_{mod} GPa	E_{mod}(10-30F_{max}) GPa
	1	2510	255,69	8,52	635,44	10,5	30000	10,99	9,25	8,23
	2	2520	256,59	8,55	623,72	10,8	30000	11,25	9,04	8,21
	3	2530	257,64	8,59	645,40	10,8	30000	11,25	9,20	8,42
	4	2500	255,26	8,51	618,74	10,5	30000	10,99	9,35	8,14
	5	2480	252,69	8,42	635,93	10,5	30000	10,97	8,94	8,20
	6	2500	255,14	8,50	639,19	10,4	30000	10,94	9,01	8,35
	7	2520	256,60	8,55	640,54	10,6	30000	11,09	9,16	8,31
	8	2550	259,80	8,66	627,27	10,7	30000	11,24	9,08	8,24
	9	2460	250,89	8,36	632,43	10,3	30000	10,91	8,99	8,23
	10	2500	255,39	8,51	619,11	10,5	30000	11,03	8,90	8,21

Statistics:

Series n = 10	F_{max} N	F_{max} kg	σ g/den	σ MPa	dL at F_{max} %	Titer den	t_{test} s	E_{mod} GPa	E_{mod}(10-30F_{max}) GPa
$\bar{x}$	2510	255,57	8,52	631,77	10,6	30000	11,07	9,09	8,25
s	24,2	2,47	0,08	6,54	0,2	0,000	0,13	0,146	0,11
V [%]	0,97	0,97	0,97	0,97	1,51	0,00	1,21	1,61	1,37

b

Table 5. Results of F-10 and F-15 yarn samples according to ISO 2062 standard

Legend	No.	F_{maxN} N	F_{maxkg} kg	$\sigma_{g/den}$ g/den	σ_{MPa} MPa	dL at F_{max} %	Titer den	t_{Test} s	E_{mod} GPa	$E_{mod(\%10-\%30Fmax)}$ GPa
	1	2210	225,30	7,51	614,24	9,9	30000	10,25	8,25	8,37
	2	2180	221,80	7,39	597,18	9,5	30000	9,89	8,40	7,84
	3	2190	223,19	7,44	601,47	9,9	30000	10,30	7,86	8,07
	4	2230	227,08	7,57	621,14	9,8	30000	10,25	8,38	8,24
	5	2190	223,16	7,44	604,84	9,7	30000	10,22	8,33	8,19
	6	2220	226,42	7,55	589,70	10,0	30000	10,40	7,95	7,74
	7	2180	222,03	7,40	609,81	9,8	30000	10,18	8,09	8,13
	8	2210	225,37	7,51	603,44	10,1	30000	10,47	7,99	8,10
	9	2180	222,05	7,40	593,15	9,8	30000	10,22	7,89	7,85
	10	2180	222,23	7,41	610,16	10,0	30000	10,39	7,83	8,39

Statistics:

Series n = 10	F_{maxN} N	F_{maxkg} kg	$\sigma_{g/den}$ g/den	σ_{MPa} MPa	dL at F_{max} %	Titer den	t_{Test} s	E_{mod} GPa	$E_{mod(\%10-\%30Fmax)}$ GPa
x̄	2200	223,86	7,46	604,51	9,8	30000	10,26	8,10	8,09
s	19,5	1,99	0,07	5,42	0,2	0,000	0,16	0,225	0,17
V [%]	0,89	0,89	0,89	0,89	1,82	0,00	1,55	2,78	2,16

a

Legend	No.	F_{maxN} N	F_{maxkg} kg	$\sigma_{g/den}$ g/den	σ_{MPa} MPa	dL at F_{max} %	Titer den	t_{Test} s	E_{mod} GPa	$E_{mod(\%10-\%30Fmax)}$ GPa
	1	2180	221,80	7,39	594,31	9,5	30000	9,89	8,26	7,21
	2	2190	223,19	7,44	603,16	9,9	30000	10,30	7,73	8,17
	3	2190	223,16	7,44	585,17	9,7	30000	10,22	8,20	7,43
	4	2170	220,93	7,36	594,44	9,7	30000	10,09	7,95	7,57
	5	2220	226,42	7,55	603,81	10,0	30000	10,40	7,82	8,11
	6	2180	222,03	7,40	601,77	9,8	30000	10,18	7,95	8,27
	7	2210	225,37	7,51	597,11	10,1	30000	10,47	7,85	7,82
	8	2180	222,05	7,40	590,82	9,8	30000	10,22	7,76	8,19
	9	2180	222,23	7,41	596,34	10,0	30000	10,39	7,69	7,97
	10	2160	220,59	7,35	602,57	9,9	30000	10,25	7,73	8,02

Statistics:

Series n = 10	F_{maxN} N	F_{maxkg} kg	$\sigma_{g/den}$ g/den	σ_{MPa} MPa	dL at F_{max} %	Titer den	t_{Test} s	E_{mod} GPa	$E_{mod(\%10-\%30Fmax)}$ GPa
x̄	2180	222,78	7,43	596,95	9,8	30000	10,24	7,89	7,87
s	18,1	1,85	0,06	4,95	0,2	0,000	0,17	0,198	0,14
V [%]	0,83	0,83	0,83	0,83	1,89	0,00	1,64	2,51	1,78

b

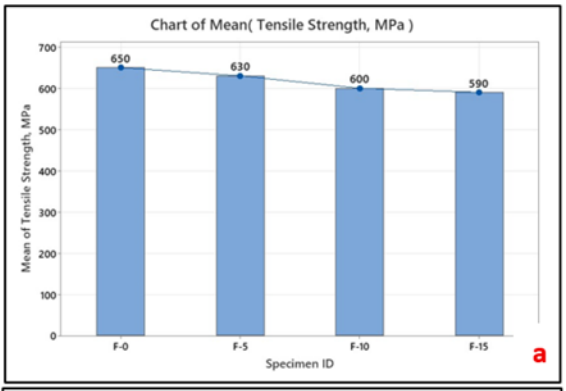

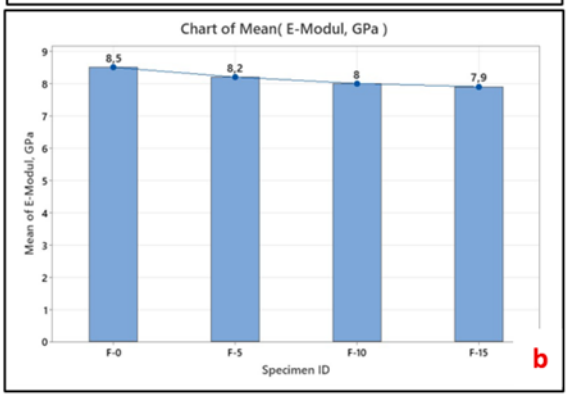

Figure 11. Tensile stress variation with granule rat and elasticity mode change with dosage-granule ratio

4. Microstructural Analysis

SEM analyses revealed that PF containing recycled granules exhibited a loss of surface homogeneity and microstructural irregularities. While the reference sample displayed a smoother and more continuous surface (Figure 12), the recycled fibers showed micro-voids and discontinuities along the fiber–matrix interface (Figure 13). This observation indicates that increasing the recycling ratio weakens the fiber–matrix interaction. In PF, the interface appeared more compact and homogeneous, whereas fibers containing recycled material exhibited increased roughness, surface heterogeneity, and interfacial discontinuities [30].

The surface irregularities observed in the recycled fibers are the primary factors that reduce interfacial adhesion at the microscopic level [31]. Chain scissions in the polymer structure, oxidative degradation, and additive residues generate micro-roughness and melting anomalies on the fiber surface. These anomalies hinder the complete contact between the cement matrix and the fiber surface, leading to micro-voids and low-density interfacial transition zones. Consequently, these defects directly contribute to the reduction of mechanical properties (Figure 14).

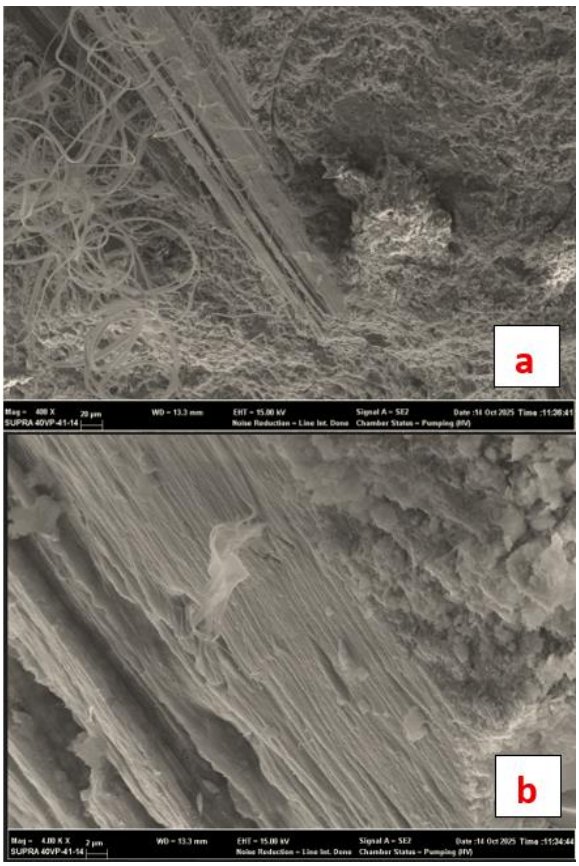

Figure 12. Non-recycled fiber appearance in sample F03 (a. 400 and b. 4K)

Figure 13. Recycled fiber appearance in sample F10-2 (400 and 4K)

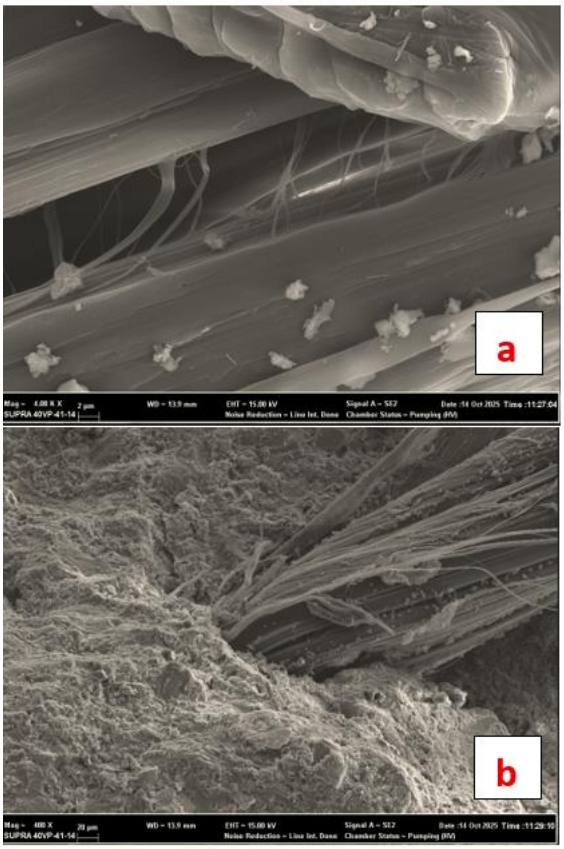

Figure 14. Recycled fiber appearance in sample F10-3 (400 and 4K)

5. Conclusion

This study investigated the effects of various proportions of recycled granule (0%, 5%, 10%, and 15%) and fiber dosage (2 kg/m³ and 3 kg/m³) used in fibers used in field concrete on the mechanical performance of concrete. The average residual strength values (fr1), (fr4), and moment coefficients obtained from the experimental data were evaluated graphically.

The results show that the fiber addition provides significant improvements in the post-cracking behavior of concrete. At all recycling ratios, the 3 kg/m³ fiber dosage produced higher fr1, fr4, and moment coefficient values compared to the 2 kg/m³ dosage. This demonstrates that the tensile ductility and energy absorption capacity of the concrete increase with increasing fiber content.

However, a significant decrease in both fr1 and fr4 values was observed as the recycled granule ratio increased. Particularly at 10% and 15% recycling rates, the adhesion capacity of the fibers to the concrete matrix decreased, resulting in a decrease in post-crack strength. This resulted

in a loss of performance due to the second heat treatment of the recycled granules.

When the moment coefficient calculation was examined, it was seen that as the recycling rate increased, the stiffness and toughness values contributing to flexural strength decreased. The highest average moment coefficient value was0.32 for the 0% recycled sample with 3 kg/m³ fiber. The lowest value was 0.18 for the 15% recycled sample with 2 kg/m³ fiber.

Consequently, it was observed that the mechanical benefits obtained from fiber addition in concrete decreased as the recycled granule ratio increased. However, this loss remained limited in mixtures up to 5% recycling rates, and the concrete's performance remained acceptable from an engineering perspective. This demonstrates that the use of recycled fibers is appropriate for sustainable material use. We observe that when the recycling rate is maintained between 0% and 5%, the effect on the mechanical performance of concrete is acceptable.

In this study, the granule content used in waste fiber production (0% → 15%) caused a decrease in both tensile strength and modulus of elasticity. While the reference sample (F-0) exhibited the highest mechanical performance, a 5% granule dosage (F-5) appears to be the optimal starting point in terms of the performance-sustainability balance. There is a decrease in mechanical properties at 10% and especially 15% dosages. SEM images, XRD, and porosity measurements, as well as examination of the granule-matrix interface, will confirm the weakening mechanism.

Article information form should be written after the Conclusion section.

Article Information Form

Acknowledgments
Authors would like to thank Polyfibers Company for their contributions.

Publications produced from theses can be listed in this section.

Authors' Contribution
Samed Demirhan performed the experimental studies, analyzed the data, and prepared the thesis work forming the basis of this article. Aylin Özodabaş conceptualized the study, structured and wrote the manuscript based on the thesis results, and finalized the paper for publication.

The Declaration of Conflict of Interest/ Common Interest
The authors declare that there is no conflict of interest or common interest related to this work.

Artificial Intelligence Statement
No artificial intelligence tools were used while writing this article. (If an artificial intelligence tool was used, please write a detailed explanation.)

References

[1] A. Geremew, A. Outtier, P. De Winne, T. A. Demissie, H. De Backer, "An experimental investigation on the effect of incorporating natural fibers on the mechanical and durability properties of concrete by using treated hybrid fiber-reinforced concrete application," Fibers, vol. 13, no. 3, pp. 26, 2025.

[2] Z. F. Akbulut, T. A. Tawfik, P. Smarzewski, S. Guler, "Advancing hybrid fiber-reinforced concrete: Performance, crack resistance mechanism, and future innovations," Buildings, vol. 15, no. 8, pp. 1247, 2025.

[3] S. Marinelli, M. A. Butturi, B. Rimini, R. Gamberini, M. A. Sellitto, "Estimating the circularity performance of an emerging industrial symbiosis network: The case of recycled plastic fibers in reinforced concrete," Sustainability, vol. 13, no. 18, pp. 10257, 2021.

[4] H. J. B. da Silva Bezerra, A. C. de Paula, J. N. de Paula et al., “Utilization of recycled synthetic fibers in concrete with a focus on structural properties enhancement: A critical literature review,” Discover Materials, vol. 4, pp. 77, 2024.

[5] A. Caggiano, P. Folino, C. Lima, E. Martinelli, M. Pepe, “On the mechanical response of hybrid fiber reinforced concrete with recycled and industrial steel fibers,” Construction and Building Materials, vol. 147, pp. 286–295, 2017.

[6] K. Liew, A. Akbar, “The recent progress of recycled steel fiber reinforced concrete,” Construction and Building Materials, vol. 232, pp. 117232, 2020.

[7] T. F. Awolusi, O. L. Oke, O. D. Atoyebi, O. O. Akinkurolere, A. O. Sojobi, “Waste tires steel fiber in concrete: a review,” Innovative Infrastructure Solutions, vol. 6, pp. 1–12, 2021.

[8] J. Ahmad, Z. Zhou, “Mechanical properties of natural as well as synthetic fiber reinforced concrete: A review,” Construction and Building Materials, vol. 333, pp. 127353, 2022.

[9] A. A. Del Savio, D. L. T. Esquivel, F. de Andrade Silva, J. Agreda Pastor, “Influence of synthetic fibers on the flexural properties of concrete: Prediction of toughness as a function of volume, slenderness ratio and elastic modulus of fibers,” Polymers, vol. 15, no. 4, pp. 909, 2023.

[10] A. H. Jin, J. S. Woo, H. D. Yun, S. W. Kim, W. S. Park, W. C. Choi, “Influence of concrete strength and fiber properties on residual flexural strength of steel fiber-reinforced concrete,” Construction and Building Materials, vol. 489, pp. 142366, 2025.

[11] A. Balea, E. Fuente, M. C. Monte, A. Blanco, C. Negro, “Recycled fibers for sustainable hybrid fiber cement-based material: a review,” Materials, vol. 14, no. 9, pp. 2408, 2021.

[12] C. Signorini, V. Volpini, “Mechanical performance of fiber reinforced cement composites including fully-recycled plastic fibers,” Fibers, vol. 9, no. 3, pp. 16, 2021.

[13] G. Liu, N. Tošić, A. de la Fuente, “Recycling of Macro-Synthetic Fiber-Reinforced Concrete and Properties of New Concretes with Recycled Aggregate and Recovered Fibers,” Applied Sciences, vol. 13, no. 4, pp. 2029, 2023.

[14] T. A. Fode, Y. A. C. Jande, T. Kivevele, “Physical, mechanical, and durability properties of concrete containing different waste synthetic fibers for green environment – A critical review,” Heliyon, vol. 10, no. 12, makale e32950, 30 Haz. 2024.

[15] M. Małek, M. Jackowski, W. Łasica, M. Kadela, “Characteristics of recycled polypropylene fibers as an addition to concrete fabrication based on Portland cement,” Materials (Basel), vol. 13, no. 8, pp. 1827, 2020.

[16] S. A. Khan, “Enhancing the mechanical properties of fiber-reinforced concrete through sustainable mix design: effects of fiber type and dose,” Discover Civil Engineering, vol. 1, pp. 88, 2024.

[17] R. Abousnina, S. Premasiri, V. Anise, W. Lokuge, V. Vimonsatit, W. Ferdous, O. Alajarmeh, “Mechanical properties of macro polypropylene fiber-reinforced concrete,” Polymers, vol. 13, no. 23, pp. 4112, 2021.

[18] J. A. Sainz-Aja, M. Sanchez, L. Gonzalez, P. Tamayo, G. Garcia del Angel, A. Aghajanian, S. Diego, C. Thomas, “Recycled polyethylene fibers for structural concrete,” Applied Sciences, vol. 12, no. 6, pp. 2867, 2022.

[19] M. Caballero-Jorna, M. Roig-Flores, P. Serna, “A study of the flexural behavior of fiber-reinforced concretes exposed to moderate temperatures,” Materials (Basel), cilt 14, sayı 13, s. 3522, 2021.

[20] EN 14651 Test method for metallic fiber concrete. Measuring the flexural tensile strength (limit of proportionality (LOP), residual).

[21] Hoque, M. A., Sultana, S., Sarker, M. K. U. & Islam, Z. (2023). Recycling Waste Polypropylene to Produce New Composite Materials with Jute Reinforcements. Advances in Materials Science, 23(3), 21–32.

[22] TS EN 934-2 Kimyasal Katkılar- Beton, Harç ve Şerbet İçin Beton Katkıları

[23] TS EN 12350-2 Beton-Taze Beton Testleri-Bölüm 2: Slump test.

[24] TS 3114 Beton Basınç Dayanımı Deney Yöntemi.

[25] M. Małek, M. Jackowski, W. Łasica, M. Kadela, “Characteristics of recycled polypropylene fibers as an addition to concrete fabrication based on Portland cement,” Materials (Basel), vol. 13, no. 8, pp. 1827, 2020.

[26] Yin, S., Tuladhar, R., Collister, T., Combe, M., Sivakugan, N., & Deng, Z. (2015). *Post-cracking performance of recycled polypropylene fiber in concrete*. Construction and Building Materials, 101, 106–113.

[27] Q. Fu, Z. Zhang, W. Xu, X. Zhao, L. Zhang, Y. Wang, D. Niu, “Flexural behavior and prediction model of basalt fiber/polypropylene fiber-reinforced concrete,” International Journal of Concrete Structures and Materials, vol. 16, sayı 31, 2022.

[28] Yin, S., Shi, C., Tuladhar, R., Rabin, R., Riella, J., Jacob, M., Chung, D., Collister, T., Combe, M., & Sivakugan, S. Comparative evaluation of virgin and recycled polypropylene fiber reinforced concrete. Construction and Building Materials, 114, 134–141., 2016

[29] ISO 2062 Tekstil- Paketlerden alınan Tekstil- Tek ipliğin kopma kuvvetinin ve Kopma anındaki uzamasının sabit hızlı uzama cihazı (CRE) kullanılarak tayini (ISO 2062:2009).

[30] T. Zhiltsova, M. S. A. Oliveira, “Sustainable polypropylene blends: balancing recycled content with processability and performance,” Polymers (Basel), cilt 17, sayı 11, s. 1556, 2025

[31] D. T. Burn, L. T. Harper, M. Johnson, N. A. Warrior, U. Nagel, L. Yang, J. Thomason, “The usability of recycled carbon fibers in short fiber thermoplastics: interfacial properties,” Journal of Materials Science, vol. 51, no. 16, pp. 7699–7715, 201